Chemical Engineering Journal 148 (2009) 263–269

Contents lists available at ScienceDirect

Chemical Engineering Journal

journal homepage: www.elsevier.com/locate/cej

Preparation, characterization and photocatalytic activity of N-containing ZnO powder

Chen Shifu*, Zhao Wei*, Zhang Sujuan, Liu Wei

Department of Chemistry, Huaibei Coal Normal College, Anhui, Huaibei 235000, People's Republic of China

ARTICLE INFO

Article history:
Received 22 June 2008
Received in revised form 18 August 2008
Accepted 25 August 2008

Keywords:
N-containing ZnO powder
Photocatalyst
Heat treatment
Activity
Characterization

ABSTRACT

N-containing ZnO photocatalyst was prepared by decomposition of zinc nitrate at different heat treatment conditions. The photocatalyst was characterized by DRS, XRD, TG-DTA, XPS, and BET analysis. The results show that the optimum preparation condition for N-containing ZnO is at 350 °C for 3 h, and the sample shows higher photocatalytic activity. The photo-absorption wavelength range of the samples is shifted to long wavelength. Compared with pure ZnO, the samples show higher visible-light photocatalytic activity. However, under UV irradiation, the photocatalytic reduction activity of the N-containing ZnO is higher than that of pure ZnO, and the photocatalytic oxidation activity of the N-containing ZnO is much lower than that of pure ZnO. It is proposed that the change of photocatalytic activity of the sample should be attributed to the nitrogen introduction. The doped nitrogen atoms in a ZnO crystal lattice will probably cause the conductivity conversion of the sample from n-type to p-type.

1. Introduction

ZnO has been widely used as a photocatalyst, owing to its high activity, low cost and environmentally friendly feature [1–7]. However, the photocatalytic activity of ZnO is limited to irradiation wavelengths in the UV region because ZnO semiconductor has a wide band-gap of about 3.2 eV and can only absorb UV light with wavelengths below 387 nm. Some problems still remain to be solved in its application, such as the fast recombination of photogenerated electron–hole pairs. Therefore, improving photocatalytic activity by modification has become a hot topic among researchers in recent years [8,9]. Changing the optical absorption properties will be necessary to attain this goal. One successful approach is to dope transition metal ions into a semiconductor photocatalyst by ion implantation or co-precipitation [10–13]. The other approach is to dope non-metallic elements such as nitrogen, fluorine, sulfur, carbon, etc. into the substitutional sites in the crystal structure of a photocatalyst [14,15]. It was reported that N-doping into the substitutional sites of TiO_2, Ta_2O_5, or $LaTaO_4$ by calcination in an NH_3 or N_2 atmosphere is effective for band-gap narrowing and visible-light photocatalysis [16–18]. Similar results are also expected for ZnO since it has almost the same band-gap energy as TiO_2.

Recently, nitrogen-doped ZnO sample has been synthesized by grinding the ZnO and urea mixture and the subsequent calcination at 400 °C [19]. The synthesized sample has exhibited photo-absorption in the region of visible-light wavelength. In addition, the sample has shown excellent photocatalytic ability. Li and Haneda [20] synthesized colored N-containing ZnO powder with high surface area. Ultraviolet–visible spectra indicated that the photocatalyst powder could absorb not only ultraviolet light like pure ZnO powder, but also part of the visible-light. The photocatalytic performance of N-containing ZnO powder was superior to that of a pure ZnO sample under visible-light irradiation. Additionally, a visible-light absorption feature was also observed on N-doped ZnO thin films [21]. These results indicated that the doped nitrogen atoms in a ZnO crystal lattice could significantly improve the optical absorption properties of ZnO.

However, for the nitrogen-doped zinc oxide and nitrogen-doped titanium dioxide photocatalysts [16–21], the photocatalytic oxidation activity of the photocatalysts was studied extensively, while the photocatalytic reduction activity of the photocatalyst was rarely reported. The results showed that, when the doped nitrogen content is higher than a certain amount, the photocatalytic oxidation activity of the photocatalysts will reduce gradually. In this paper, N-containing ZnO was prepared by means of a novel, quick and simple method. The photocatalytic activity of the photocatalyst was evaluated comprehensively by photocatalytic reduction of $Cr_2O_7^{2-}$ and photocatalytic oxidation of methyl orange (MO) under both UV and visible-light irradiation. A significant result was obtained. Namely, under UV irradiation, the photocatalytic reduction activity of the N-containing ZnO is higher than that of pure ZnO, and the photocatalytic oxidation activity of the N-containing ZnO is much lower than that of pure ZnO. The effect of the heat treatment condition on the photocatalytic activity of the photocatalyst was investigated.

* Corresponding authors. Tel.: +86 561 3806611; fax: +86 561 3803141.
E-mail address: chshifu@hbcnc.edu.cn (C. Shifu).

1385-8947/$ – see front matter © 2008 Elsevier B.V. All rights reserved.
doi:10.1016/j.cej.2008.08.039

The possible mechanisms for the change of photocatalytic activity of the sample were also investigated.

2. Experimental

2.1. Materials

Zinc nitrate [$Zn(NO_3)_2{\cdot}6H_2O$] (purity 99.9%), pure ZnO (crystallite size is about 30 nm), ethyl alcohol, potassium dichromate ($K_2Cr_2O_7$), methyl orange (MO), and other chemicals used in the experiments were of analytically pure grade. They were purchased from Shanghai and other China Chemical Reagent Ltd. without further purification. Deionized water was used throughout this study.

2.2. Preparation of N-containing ZnO powder

Zinc nitrate [$Zn(NO_3)_2{\cdot}6H_2O$] was heated at a heating rate of 10 °C/min in air to prepare N-containing ZnO powder. Nitrate first melts at 36 °C, and then dehydrates just above 100 °C. Nitrate decomposition completes at about 350 °C. The synthesized N-containing ZnO powder was ground in the agate ball milling tank. In order to study the effect of the heat treatment condition on the photocatalytic activity of the photocatalyst, N-containing ZnO powder was prepared by decomposition of zinc nitrate at different heat treatment temperatures and time. The powders were vivid and darkish yellow in color under the preparation conditions.

2.3. Photoreactor and procedure

Experiments were carried out in a photoreaction apparatus. The schematic diagram is shown in Fig. 1. The apparatus consists of two parts. The first part is an annular quartz tube. A 375 W medium pressure mercury lamp (Institute of Electric Light Source, Beijing) with a maximum emission at about 365 nm and a 500 W Xe lamp (Institute of Electric Light Source, Beijing) with a maximum emission at about 470 nm were used as UV and visible-light sources, respectively. The wavelength of the visible-light is controlled through a 420 nm cut filter (Instrument Company of Nantong, China). The lamp is laid in the empty chamber of the annular quartz tube, and running water passes through an inner thimble of the annular tube. Owing to continuous cooling, the temperature of the reaction solution is maintained at approximately 30 °C. The second part is an unsealed beaker of a diameter 12 cm. At the start of the experiment, the reaction solution (volume, 300 cm^3) containing reactants and photocatalyst was put in the unsealed beakers, and a magneton was used to stir the reaction solution. The distance between the light source and the surface of the reaction solution is 11 cm. In the experiment, the initial pH of the reaction solution was about 5.0. The amount of photocatalyst used was 2.0 g L^{-1}; the initial concentrations of $Cr_2O_7^{2-}$ and methyl orange (MO) were 2.9×10^{-4} and 1.0×10^{-4} mol L^{-1}, respectively. The illumination time of each experiment was 20 min. In order to disperse the photocatalyst powder, the suspensions were ultrasonically vibrated for 20 min prior to irradiation. After the illumination, the samples (volume of each is 5 cm^3) were taken from the reaction suspension, centrifuged at 7000 rpm for 10 min and filtered through a 0.2 μm Millipore filter to remove the particles. The filtrate was then analyzed. In order to determine the reproducibility of the results, at least duplicated runs were carried out for each condition for averaging the results. The blank test was also carried out by irradiating MO (or $Cr_2O_7^{2-}$) homogeneous solution without photocatalyst under both UV and visible-light irradiation for checking the photo-induced self-sensitized photodegradation.

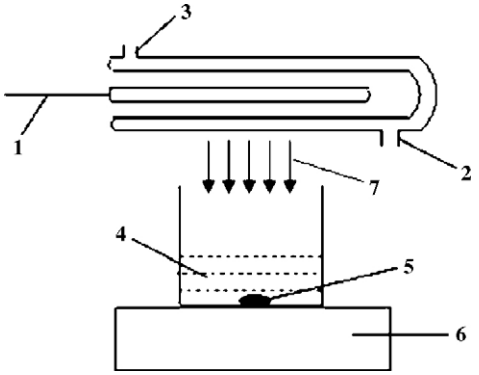

Fig. 1. Schematic diagram of photoreaction apparatus: 1, lamp; 2, water-cooling inlet; 3, water-cooling outlet; 4, reaction solution; 5, stirring rod; 6, magnetic agitator; 7, light.

2.4. Characterization

UV–vis diffuse reflectance spectroscopy (DRS) measurements were carried out using a Hitachi UV-365 spectrophotometer equipped with an integrating sphere attachment. The analysis range was from 300 to 650 nm, and $BaSO_4$ was used as a reflectance standard.

In order to determine the crystal phase composition and the crystallite size of the photocatalysts, X-ray diffraction (XRD) measurement was carried out at room temperature using a DX-2000 X-ray powder diffractometer with Cu Kα radiation and a scanning speed of 3°/min. The accelerating voltage and emission current were 40 kV and 30 mA, respectively. The crystallite size was calculated by X-ray line broadening analysis using the Scherrer equation.

The specific surface area (BET) was determined by N_2 adsorption–desorption isotherms at liquid nitrogen temperature (77 K) using a Quantachrome NOVA 2000e adsorption instrument. Thermogravimetric (TG) and differential thermal analysis (DTA) of the precursor were carried out at a heating rate of 10 °C/min in static air (TA Instruments, SDT 2960, USA).

X-ray photoelectron spectroscopic (XPS) examination was carried out on a Thermo ESCALAB 250 multifunctional spectrometer (VG Scientific UK) using Al Kα radiation. All XPS spectra were referenced to the C 1s peak at 284.8 eV from the adventitious hydrocarbon contamination.

2.5. Analysis

The concentration of $Cr_2O_7^{2-}$ in solution was determined by spectrophotometer using diphenylcarbazide reagent as a developer. The concentration of MO in solution was determined by spectrophotometer.

The photoreduction efficiency of $Cr_2O_7^{2-}$ and the photoxidation efficiency of MO were calculated from the following expression:

$$\eta\% = \frac{(C_0 - C_t)}{C_0} \times 100$$

where η is the photocatalytic efficiency; C_0 is the initial concentration of reactant; C_t is the concentration of reactant after illumination time t.

3. Results and discussion

3.1. Characterization of N-containing ZnO photocatalyst

3.1.1. TG-DTA analysis

The simultaneous TG-DTA curves of zinc nitrate [$Zn(NO_3)_2{\cdot}6H_2O$] are shown in Fig. 2, The strong endothermic

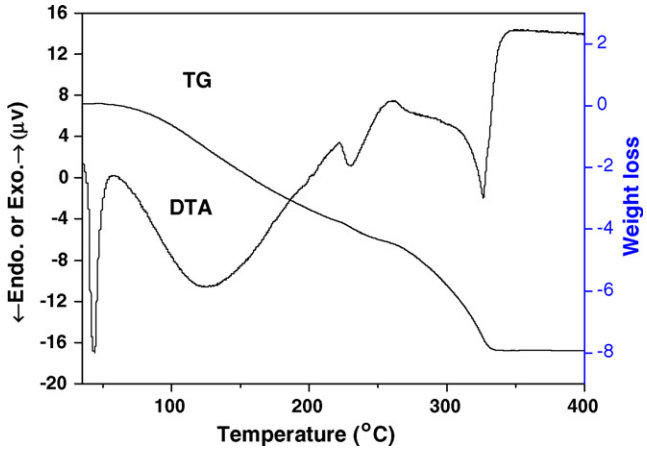

Fig. 2. TG-DTA curve of $Zn(NO_3)_2{\cdot}6H_2O$.

DTA peak can be clearly seen at about 42.6 °C; the weight loss does not occur in the temperature range, which corresponds to the crystal water melting of zinc nitrate. The TG curve shows that thermal decomposition of the zinc nitrate at temperatures below 350 °C proceeds via two steps. The first step starts at about 56.8 °C, with a broad endothermic DTA peak centered at 125.7 °C and a little endothermic DTA peak centered at about 230 °C. It is attributed to the partial dehydration of $Zn(NO_3)_2{\cdot}6H_2O$ and thermal decomposition to basic zinc nitrate of variable composition. The second step takes place between 258.2 and 344.1 °C, corresponding to the decomposition of the intermediates to ZnO [22]. From the results of TG analysis, it is known that $Zn(NO_3)_2{\cdot}6H_2O$ can be decomposed completely into ZnO below 350 °C.

3.1.2. XPS analysis

Fig. 3 shows higher resolution scanning XPS spectra of Zn 2p of pure ZnO and Zn 2p, N 1s, O 1s of the sample, respectively. The sample was prepared at 350 °C for 3 h.

From the higher resolution scanning XPS spectra of Zn $2p_3$, it can be seen that, the photoelectron peak of the sample for Zn $2p_3$ appears clearly at the binding energy of 1022.5 eV. And for pure ZnO, the binding energy of Zn $2p_3$ is at 1021.5 eV. At the same time, it has been reported that, for undoped nitrogen ZnO, the photoelectron peak for Zn $2p_3$ appears at the binding energy of 1021.4 eV [23,24]. It is clear that the peak is shifted toward higher binding energy in Zn $2p_3$ spectrum of N-containing ZnO as compared with that of the undoped nitrogen ZnO. Lin et al. [25] assigned this peak shift to the reduction of the surface band bending, and this may be related to the doping or incorporation of N ions into ZnO powders. The doped nitrogen atoms could have the probability to occupy O sites to form the acceptor (N_O) in ZnO powders.

From high resolution scanning XPS spectra of O 1s in Fig. 3, it can be seen that oxygen on the sample surface exists at least in three forms with the following binding energies: 530.4, 532 and 533.5 eV. The peak at 530.4 eV is mainly assigned to the oxygen atoms coordinated with Zn atoms [26]. The peak at 532 eV corresponds to oxygen in the sample surface adsorption of (–OH) [27,28]. The peak at 533.5 eV is likely due to irreversibly adsorbed water molecules on the surface [29–31]. It is just because so much adsorption oxygen exists on the sample surface that they become captives of photo-generated electron–hole pairs directly or indirectly. Therefore, recombination of the photo-generated electron–hole pairs is suppressed, and the quantum efficiency of photocatalytic reaction is improved [30].

From the higher resolution scanning XPS spectra of N 1s, it can be seen that there are nitrogen signals in the sample, though

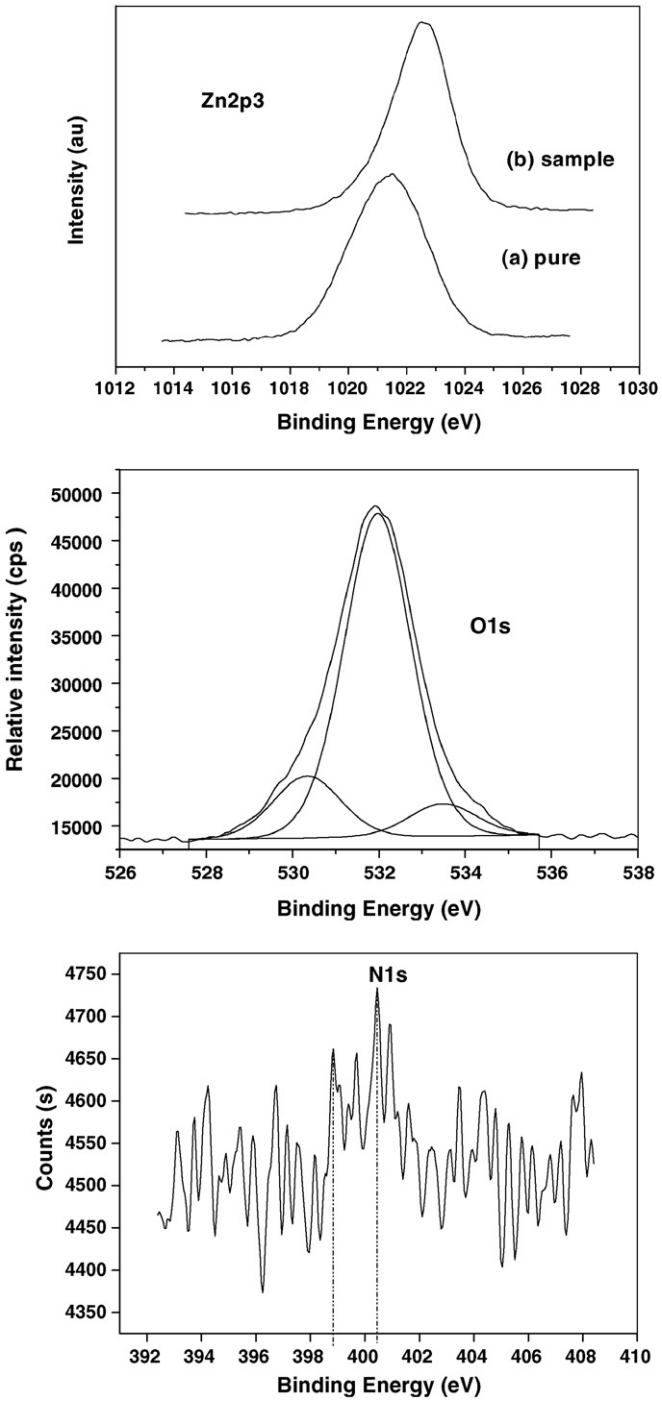

Fig. 3. High resolution scanning XPS spectra of Zn $2p_3$, O 1s, and N 1s.

the peak intensity is not strong. The amount of nitrogen is about 1.0 at.%. It is known that, the binding energy assignment for N–Zn bonds seems still very controversial. Ma et al. reported a binding energy of 396.2 eV for N–Zn bonds in N-doped ZnO by radio frequency reactive magnetron sputtering [32], while Joseph et al. reported 397.84 eV for N–Zn bonds in (N, Ga)-co-doped ZnO films and 406.5 eV in N alone doped ZnO [33]. In Maki's work, the peaks around 398 eV attributed to Zn–N bond were observed in the N-doped ZnO single crystal [34]. Based on these previous works and analysis, it is proposed that the binding energy peak at 398.8 eV corresponds to nitrogen substitution on the oxygen sublattice (N_O),

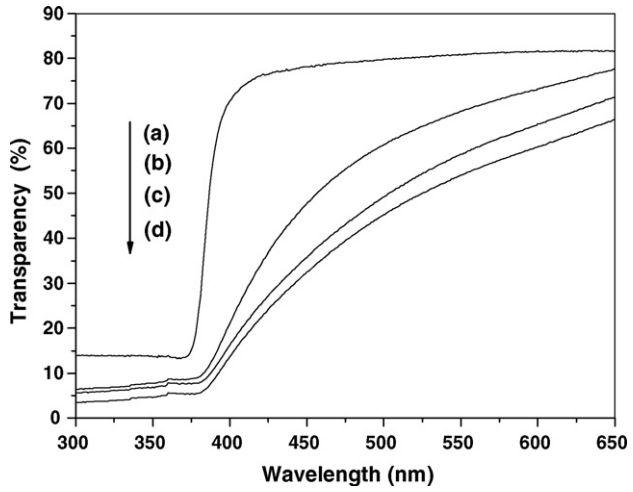

Fig. 4. UV–vis diffuse reflection spectra of the samples: (a) pure ZnO, (b) 300 °C, (c) 400 °C and (d) 350 °C.

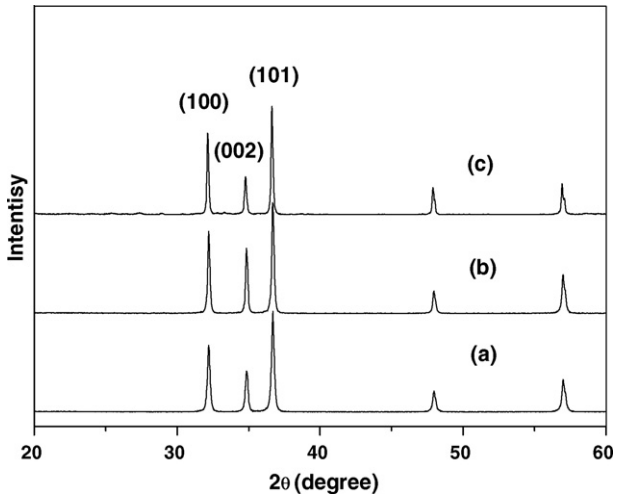

Fig. 5. XRD patterns of N-containing ZnO prepared at different temperatures for 3 h. (a) 300 °C, (b) 350 °C and (c) 400 °C.

the desired location for p-type doping. Asahi et al. [14] proposed that the substitutional N (N_O) may be related to the active sites for the photocatalysis. The binding energy peak at 400.5 eV is likely assigned to N–O bond in the sample surface adsorption of NO_x compound [35].

3.1.3. UV–vis analysis

Fig. 4 shows UV–vis diffuse reflection spectra of N-containing ZnO and pure ZnO powder. The N-containing ZnO powders were prepared at different heat treatment temperatures for 3 h.

From Fig. 4, it is clear that the absorption wavelength range of N-containing ZnO powder is shifted to long wavelength, compared with pure ZnO powder, and its absorption intensity is also increased. The absorption in the visible range can be attributed to the nitrogen doping. Li and Haneda [20] assigned the mentioned absorption to the nitrogen atoms doped into the oxygen sites of the ZnO crystal lattice.

From Fig. 4, it also can be seen that, N-containing ZnO powder prepared at 350 °C has maximum absorption intensity, followed by those that were prepared at 400 and 300 °C. It is clear that the absorption intensity of samples depends on the heat treatment temperatures. Generally, a higher nitrogen concentration should be expected since the Vis photocatalytic activity depends on the concentration of doped nitrogen. It is natural that higher heat treatment temperature gives lower nitrogen content since nitrogen burns away. However, N-doping cannot occur wholly at a lower heat treatment temperature owing to the uncompleted decomposition of precursor (zinc nitrate). This analysis coincides with the TG-DTA curves of zinc nitrate. It is clear that the higher nitrogen concentration should be fulfilled through heat treatment at a moderate temperature. It explains why the absorption intensity of N-containing ZnO reaches a maximum at 350 °C. It also agrees with the result of the photocatalytic activity under visible-light irradiation.

3.1.4. XRD and BET analysis

Heat treatment is a common method that can be used to improve the crystallinity and photocatalytic activities of photocatalyst. Figs. 5 and 6 show the XRD patterns of photocatalysts prepared at different heat treatment temperatures and time. It can be seen that N-containing ZnO powder exhibits dominant diffraction peaks of wurtzite phase.

Fig. 5 shows XRD patterns for N-containing ZnO powder prepared at temperatures from 300 to 400 °C. A clear sharpening and attenuation of the peaks can be observed as the temperature increases, indicating that the crystallinity of the photocatalyst increases with the increase of heat treatment temperature. From the results of TG-DTA, when the N-containing ZnO powder was prepared at lower temperatures, zinc nitrate cannot be decomposed completely into ZnO, and a few amounts of amorphous phase still remain in this sample. However, from Fig. 5, it is clear that XRD pattern of the sample prepared at 300 °C does not have obvious amorphous phase. Fig. 6 shows XRD patterns of N-containing ZnO powder prepared at 350 °C for different heat treatment time. From Fig. 6, it also can be seen that the crystallinity of the photocatalyst increases with the increase of heat treatment time.

Crystallite sizes of the N-containing ZnO were calculated from the X-ray peak broadening of the (1 0 1) diffraction peak using the Scherrer formula [36]. The crystal sizes of N-containing ZnO are shown in Table 1. It can be seen from Table 1 that the crystallite size of N-containing ZnO increases with the increase of heat treatment temperature from 300 to 400 °C. The crystallite size of the sample also increases with the increase of heat treatment time.

BET surface areas are also given in Table 1. From Table 1, it is known that the surface area of N-containing ZnO decreases from 28.5 to 13.9 $m^2 g^{-1}$ and the crystallite size increases from

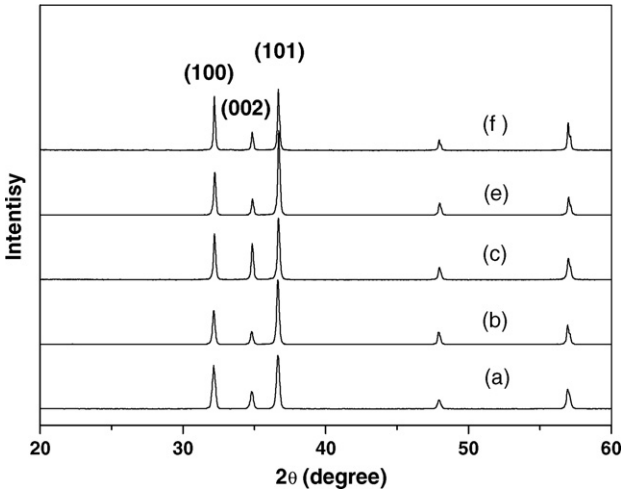

Fig. 6. XRD patterns of N-containing ZnO prepared at 350 °C for different time. (a) 1 h, (b) 2 h, (c) 3 h, (d) 5 h and (e) 7 h.

Table 1
Summary of the properties and heat treatment conditions of samples

Temperature (°C)	Time (h)	FWHM value (rad)	BET area ($m^2\ g^{-1}$)	Crystal size (nm)
300	3	0.0039	24.1	36.9
350	1	0.0044	28.5	32.9
350	2	0.0037	21.2	39.5
350	3	0.0035	20.3	40.6
350	5	0.0032	17.5	45.5
350	7	0.0029	14.8	49.0
400	3	0.0028	13.9	50.8

32.9 to 50.8 nm. This indicates that the decrease of surface area is mainly due to the growth of crystallite size. Another important reason is that with the increase in heat treatment temperature and time, the pores of N-containing ZnO powder gradually collapse, and that pore is caused by the liberation of a large amount of gases (NO_x) during the heat treatment. From Table 1, it can also be seen that FWHM value of the sample decreases as the heat treatment temperature increases. This indicates that the crystallinity of the photocatalyst improves with the increase of heat treatment temperature.

3.2. Evaluation of photocatalytic activity of N-containing ZnO powder

3.2.1. Photocatalytic activity under UV irradiation

Effects of heat treatment on the photocatalytic reduction of $Cr_2O_7^{2-}$ and the photocatalytic oxidation of MO under UV irradiation are shown in Table 2.

From Table 2, it can be seen that, when the heat treatment temperature is 350 °C, the best heat treatment time is 3 h. The photocatalytic activity of N-containing ZnO powder increases with the increase of heat treatment time up to 3 h. When the heat treatment time is longer than 3 h, the photocatalytic activity of N-containing ZnO powder decreases gradually with the increase of the heat treatment time. The photocatalytic activities of N-containing ZnO prepared at different heat treatment temperatures and time are also measured. The results show that, when the heat treatment temperature is 300 °C, the photocatalytic activity increases with the increase of heat treatment time; however, when the heat treatment temperature is 400 °C, the photocatalytic activity decreases with the increase of heat treatment time.

Ohtani et al. [37] have proposed a simple model of the photocatalytic mechanism. According to their model, a high activity of photocatalyst should satisfy two requirements, namely, large surface area for absorbing substrates and high crystallinity to reduce photo-excited electron–hole recombination rate. However, these requirements are in general conflict with each other, because the crystallinity increases with the heat treatment temperature while the surface area does decrease. When N-containing ZnO powders are prepared at temperature 300 °C, zinc nitrate is not decomposed completely into ZnO. A certain amount of amorphous N-containing ZnO still exists and acts as a site of photo-excited electron–hole recombination, which is adverse to the photocatalytic activity of N-containing ZnO. Calcination can increase the crystallinity of the sample; the crystallinity improves as the heat treatment time increases. Therefore, the longer heat treatment time exhibits an advantageous effect on the photocatalytic activity at lower temperatures. Although N-containing ZnO powder prepared at temperature 400 °C has high crystallinity, the crystal size of the sample increases with the increase of heat treatment time, and it decreases the surface area of the sample. Therefore, the long heat treatment time exhibits an adverse effect on the photocatalytic activity of high temperatures. From the above results, it is clear that the two requirements are only partially satisfied by the heat treatment at a moderate temperature. This explains why the photocatalytic activity of N-containing ZnO reaches a maximum at 350 °C for 3 h in this study. The photocatalytic activity of N-containing ZnO powder prepared in any other preparation conditions is lower than that of heat treatment at 350 °C for 3 h. It is proposed that the photocatalyst not only should have a large surface area, but also a high crystallinity in this preparation condition. It can be seen that, the heat treatment temperature and time are the important factors that influence the photocatalytic activity of N-containing ZnO powder.

Table 2
The photocatalytic activity of N-containing ZnO under UV irradiation

Calcination time (h)	1	2	3	5	7
η_1 (%)	24.7	29.3	38.9	30.2	26.7
η_2 (%)	11.4	16.3	18.2	15.7	11.6

Temperature: 350 °C η_1: $Cr_2O_7^{2-}$; η_2: methyl orange (MO).

From Table 2, it also can be seen that, when N-containing ZnO is prepared at temperature 350 °C for 3 h, the photoreduction efficiency and photo-oxidation efficiency are 38.9% and 18.2%, respectively. For comparison, the photocatalytic performance of pure ZnO is also measured. The results show that, for the pure ZnO, the photoreduction efficiency and photo-oxidation efficiency are 14.3% and 73.5%, respectively. It is clear that the photocatalytic reduction activity of N-containing ZnO is greater than that of pure ZnO. However, the photocatalytic oxidation activity of N-containing ZnO is much lower than that of pure ZnO. It is proposed that the change of photocatalytic activity of N-containing ZnO should be attributed to the nitrogen introduction. According to the first-principle calculation of nitrogen-doped ZnO [38], the doped nitrogen in zinc oxide will cause the appearance of redundant carrier-hole near the top of valence band. The mutual exclusion effect between the holes will enable the carrier to form a narrow-deep acceptor level in the energy gap, which causes the conductivity conversion of N-containing zinc oxide from n-type to p-type. The conclusion has been proved by iodometric titrations [39]. At the same time, it has also been reported that nitrogen-doped into substitutional sites of TiO_2 crystal results in the conductivity conversion of $TiO_{2-x}N_x$ photocatalyst from n-type to p-type [40]. According to the photo-electrochemistry property of semiconductor, photoexcited holes move to the interior of p-type semiconductor under irradiation, while photoexcited electrons to the surface, which is beneficial to the photoreduction reaction between photoelectrons and the substances adsorbed on the surface of the semiconductor. From the above assumption, it is clear that the doped nitrogen enhances the photocatalytic reduction activity of ZnO under UV irradiation. Zhu et al. also reported that n-type semiconductor has higher photocatalytic oxidation activity, and p-type semiconductor has higher photocatalytic reduction activity [41].

3.2.2. Photocatalytic activity under visible-light irradiation

The wavelength of the visible-light (Vis) is controlled through a 420 nm cut filter. Effects of heat treatment on the photocatalytic

Table 3
The photocatalytic activity of N-containing ZnO under visible-light irradiation

Calcination time (h)	1	2	3	5	7
η_1 (%)	18.2	21.3	29.1	25.1	21.9
η_2 (%)	9.9	14.2	16.0	13.3	9.8

Temperature: 350 °C η_1: $Cr_2O_7^{2-}$; η_2: methyl orange (MO).

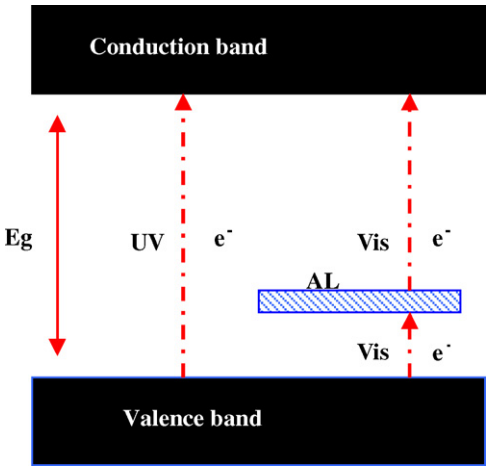

Fig. 7. Proposed energy-band structure model for N-containing ZnO.

reduction of $Cr_2O_7^{2-}$ and the photocatalytic oxidation of MO under Vis irradiation are shown in Table 3.

From Table 3, it can be seen that, the effect of heat treatment temperatures and time on the photocatalytic activities of N-containing ZnO under Vis irradiation is the same as the results under UV irradiation. The best preparation condition is also at 350 °C for 3 h. The photocatalytic activity of N-containing ZnO powder prepared in any other preparation condition is lower than that of heat treatment at 350 °C for 3 h.

From Table 3, it can also be seen that, when the N-containing ZnO photocatalyst is prepared at temperature 350 °C for 3 h, the photoreduction efficiency and photo-oxidation efficiency are 29.1% and 16.0%, respectively. It is known that the band-gap of pure ZnO is 3.2 eV, and it can be excited by photons with wavelengths below 387 nm, the pure ZnO has little activity on the photocatalytic reduction of $Cr_2O_7^{2-}$ and the photocatalytic oxidation of MO under Vis irradiation. It is clear that, the photocatalytic activity of N-containing ZnO is much higher than that of pure ZnO under visible-light irradiation.

Li and Haneda proposed a mechanism for the visible-light photocatalysis of N-containing ZnO powder [20]. The mechanism ascribes to an acceptor level, newly formed by N-doping between the conduction band (CB) and the valence band (VB) in the ZnO band structure. The proposed energy-band structure in N-containing ZnO is illustrated in Fig. 7. The electrons generated in the VB of ZnO by visible-light irradiation could have been first excited to the AL, and further transferred to the CB of ZnO. This means that the electron transition from VB to CB in a ZnO semiconductor, generally produced by UV irradiation ($h\nu > 3.2$eV), can be fulfilled through two-step transitions even with the lower energy of visible-light irradiation since an AL is formed.

4. Conclusions

N-containing ZnO photocatalyst was prepared by decomposition of zinc nitrate, which shows higher photocatalytic activity. The optimum preparation condition is at 350 °C for 3 h. Under the preparation condition, the sample not only has a large surface area, but also a high crystallinity. The absorption wavelength range of N-containing ZnO powder is shifted to long wavelength, and its absorption intensity is also increased. Doped nitrogen significantly improves the visible-light photocatalytic activity of the samples. The UV photocatalytic oxidation activity of N-containing ZnO is lower than that of pure ZnO. Nevertheless, the UV photocatalytic reduction activity of N-containing ZnO is higher than that of pure ZnO. The change of photocatalytic activity of the sample should be attributed to the nitrogen introduction, which causes the conductivity conversion of the samples from n-type to p-type.

Acknowledgements

This work was supported by the Natural Science Foundation of China (No. 20673042), the Natural Science Foundation of Anhui Province (Contract No. 070415211), the Key Project of Science and Technology Research of Ministry of Education of China (208062) and the Natural Science Foundation of Anhui Provincial Education Committee (KJ2007A015).

References

[1] N. Sobana, M. Swaminathan, The effect of operational parameters on the photocatalytic degradation of acid red 18 by ZnO, Sep. Purif. Technol. 56 (2007) 101–107.
[2] M. Mrowetz, E. Selli, Photocatalytic degradation of formic and benzoic acids and hydrogen peroxide evolution in TiO_2 and ZnO water suspensions, J. Photochem. Photobiol. A: Chem. 180 (2006) 15–22.
[3] T. Pauporte, J. Rathousky, Electrodeposited mesoporous ZnO thin films as efficient photocatalysts for the degradation of dye pollutants, J. Phys. Chem. C 111 (2007) 7639–7644.
[4] D. Li, H. Haneda, Morphologies of zinc oxide particles and their effects on photocatalysis, Chemosphere 51 (2003) 129–137.
[5] B. Dindar, S. Icli, Unusual photoreactivity of zinc oxide irradiated by concentrated sunlight, J. Photochem. Photobiol. A: Chem. 140 (2001) 263–268.
[6] J. Yu, X. Yu, Hydrothermal synthesis and photocatalytic activity of zinc oxide hollow spheres, Environ. Sci. Technol. 42 (2008) 4902–4907.
[7] V. Houskova, V. Stengl, S. Bakardjieva, N. Murafa, A. Kalendova, F. Oplustil, Zinc oxide prepared by homogeneous hydrolysis with thioacetamide, its destruction of warfare agents, and photocatalytic activity, J. Phys. Chem. A. 111 (2007) 4215–4221.
[8] Y. Zheng, L. Zheng, Y. Zhan, X. Lin, Q. Zheng, K. Wei, Ag/ZnO heterostructure nanocrystals: synthesis, characterization, and photocatalysis, Inorg. Chem. 46 (2007) 6980–6986.
[9] C. Hu, Y. Lan, J. Qu, X. Hu, A. Wang, Ag/AgBr/TiO_2 visible light photocatalyst for destruction of azo dyes and bacteria, J. Phys. Chem. B 110 (2006) 4066–4072.
[10] M. Anpo, Use of visible light second-generation titanium oxide photocatalysts prepared by the application of an advanced metal ion implantation method, Pure Appl. Chem. 72 (2000) 1787–1792.
[11] D. Dvoranová, V. Brezová, M. Mazúr, M.A. Malati, Investigations of metal-doped titanium dioxide photocatalysts, Appl. Catal. B: Environ. 37 (2002) 91–105.
[12] I. Nakamura, N. Negishi, S. Kutsuna, T. Ihara, S. Sugihara, K. Takeuchi, Role of oxygen vacancy in the plasma-treated TiO_2 photocatalyst with visible light activity for NO removal, J. Mol. Catal. A: Chem. 161 (2000) 205–212.
[13] S. Iimura, H. Teduka, A. Nakagawa, S. Yoshihara, T. Shirakashi, Improvement of the photocatalytic activity of titanium oxide by X-ray irradiation, Electrochemistry 69 (2001) 324–328.
[14] R. Asahi, T. Morikawa, T. Ohwaki, K. Aoki, Y. Taga, Visible-light photocatalysis in nitrogen-doped titanium oxides, Science 392 (2001) 269–271.
[15] M. Hara, G. Hitoki, T. Takata, J.N. Kondo, H. Kobayashi, K. Domen, TaON and Ta_3N_5 as new visible light driven photocatalysts, Catal. Today 78 (2003) 555–559.
[16] W. Balcerski, S.Y. Ryu, M.R. Hoffmann, Visible-light photoactivity of nitrogen-doped TiO_2: photo-oxidation of HCO_2H to CO_2 and H_2O, J. Phys. Chem. C 111 (2007) 15357–15362.
[17] T. Murase, H. Irie, K. Hashimoto, Visible light sensitive photocatalysts, nitrogen-doped Ta_2O_5 powders, J. Phys. Chem. B 108 (2004) 15803–15807.
[18] M. Jansen, H.P. Letschert, Inorganic yellow-red pigments without toxic metals, Nature 404 (2000) 980–982.
[19] J.F. Lu, Q.W. Zhang, J. Wang, F. Saito, M. Uchida, Synthesis of N-doped ZnO by grinding and subsequent heating ZnO–urea mixture, Powder Technol. 162 (2006) 33–37.

[20] D. Li, H. Haneda, Synthesis of nitrogen-containing ZnO powders by spray pyrolysis and their visible-light photocatalysis in gas-phase acetaldehyde decomposition, J. Photochem. Photobiol. A: Chem. 155 (2003) 171–178.
[21] X. Wang, S. Yang, J. Wang, M. Li, X. Jiang, G. Du, X. Liu, R.P.H. Chang, Nitrogen doped ZnO film grown by the plasma-assisted metal-organic chemical vapor deposition, J. Cryst. Growth 226 (2001) 123–129.
[22] M. Maneva, N. Petron, On the thermal decomposition of $Zn(NO_3)_2{\cdot}6H_2O$ and its deuterated analogue, J. Therm. Anal. 35 (1989) 2297–2303.
[23] B.F. Dzhurinskii, D. Gati, N.P. Sergushin, V.I. Nefedov, Ya.V. Salyn, Simple and coordination compounds. An X-ray photoelectron spectroscopic study of certain oxides, Russian J. Inorg. Chem. 20 (1975) 2307.
[24] L. Jing, Z. Xu, J. Shang, X. Sun, W. Cai, H. Guo, The preparation and characterization of ZnO ultrafine particles, Mater. Sci. Eng. A 332 (2002) 356–361.
[25] C.C. Lin, H.P. Chen, S.Y. Chen, Synthesis and optoelectronic of arrayed p-type ZnO nanorods grown on ZnO film/Si water in aqueous solutions, Chem. Phys. Lett. 404 (2005) 30–34.
[26] S. Anandana, A. Vinu, K.L.P. Sheeja Lovely, N. Gokulakrishnan, P. Srinivasu, T. Mori, V. Murugesan, V. Sivamurugan, K. Ariga, Photocatalytic activity of La-doped ZnO for the degradation of monocrotophos in aqueous suspension, J. Mol. Catal. A: Chem. 266 (2007) 149–157.
[27] B. Stypula, J. Stoch, The characterization of passive films on chromium electrodes by XPS, Corros. Sci. 36 (1994) 2159–2167.
[28] S.F. Chen, S.J. Zhang, W. Liu, W. Zhao, Preparation and activity evaluation of p–n junction photocatalyst NiO/TiO_2, J. Hazard. Mater. 155 (2008) 320–326.
[29] A.M. Beccaria, G. Castello, G. Poggi, Influence of passive film composition and sea water pressure on resistance to localized corrosion of some stainless steels in sea water, Br. Corros. J. 30 (1995) 283–287.
[30] S.F. Chen, L. Chen, The preparation of coupled SnO_2/TiO_2 photocatalyst by ball milling, Mater. Chem. Phys. 98 (2006) 116–120.
[31] S.F. Chen, L. Chen, The preparation of coupled WO_3/TiO_2 photocatalyst by ball milling, Powder Technol. 160 (2005) 198–202.
[32] J.G. Ma, Y.C. Liu, R. Mu, J.Y. Zhang, Y.M. Lu, D.Z. Shen, X.W. Fan, Method of control of nitrogen content in ZnO films: Structural and photoluminescence properties, J. Vac. Sci. Technol. B 22 (2004) 94–98.
[33] M. Joseph, H. Tabata, T. Kawai, p-Type electrical conduction in ZnO thin films by Ca and N codoping, Jpn. J. Appl. Phys. 38 (1999) L1205–1207.
[34] H. Maki, I. Sakaguchi, N. Ohashi, S. Sekiguchi, H. Haneda, J. Tanaka, N. Ichinose, Nitrogen ion behavior on polar surfaces of ZnO single crystals, Jpn. J. Appl. Phys. Part I 42 (2003) 75–77.
[35] K. Merritt, R.S. Wortman, M. Millard, S.A. Brown, Biomater, XPS analysis of 316 LVM corroded in serum and in saline, Med. Devices Artif. Org. 11 (1983) 115–127.
[36] H.P. Klug, L.E. Alexander, X-ray Diffraction Procedures for Polycrystalline and Amorphous Materials, Wiley, New York, 1997.
[37] B. Ohtani, Y. Ogawa, S.-I. Nishimoto, Photocatalytic activity of amorphous-anatase mixture of Titanium(IV) oxide particles suspended in aqueous solutions, J. Phys. Chem. B 101 (1997) 3746–3752.
[38] K. Chen, G.H. Fan, Y. Zhang, S.F. Ding, First-principle calculation of nitrogen-doped p-ZnO, Acta. Phys. Chim. Sin. 24 (2008) 61–66.
[39] J. Li, R. Kykyneshi, J. Tate, A.W. Sleight, p-Type zinc oxide powders, Solid State Sci. 9 (2007) 613–618.
[40] B. Gao, Y. Ma, Y. Cao, W. Yang, J. Yao, Great enhancement of photocatalytic activity of nitrogen-doped titania by coupling with tungsten oxide, J. Phys. Chem. B 110 (2006) 14391–14397.
[41] L.J. Zhu, D.J. Wang, T.F. Xie, J. Shang, Z.L. Xu, Y.G. Du, Researches on photocatalytic activities and photovoltaic properties of TiO_2 nanoparticles, Chem. J. Chin. Univ. 22 (2001) 827–829.